



## The kinetics of the simultaneous decolorization and desulfurization of azo dye wastewater in a microbial fuel cell

Xizi Long<sup>a</sup>, Chuqiao Wang<sup>b</sup>, Xian Cao<sup>c</sup>, Xianning Li<sup>a,\*</sup>

<sup>a</sup>School of Energy and Environment, Southeast University, Nanjing 210096, China, Tel. +86-15150667612, Fax +86-02583795618, email: xizi\_long@163.com (X. Long), Tel. +86 13776650963, Fax +86 025 83795618, email: lxneu@163.com (X.n. Li)

<sup>b</sup>School of Environmental and Safety Engineering, Changzhou University, Changzhou, 213164, China, Tel. +86-18795899956, email: wangchuqiao@cczu.edu.cn (C. Wang)

<sup>c</sup>Department of Civil and Environmental Engineering, Graduate School of Engineering, Tohoku University, Aoba Aramaki 6-6-06, Sendai 980-8579, Japan, Tel. +86-15905167302, email: lovevolkswagen@163.com (X. Cao)

Received 19 October 2018; Accepted 20 February 2019

### ABSTRACT

This study investigated the effects of a microbial fuel cell (MFC) on the simultaneous decolorization and desulfurization of azo dye wastewater. It showed that the conversion of sulfur at the anode had a significant effect on electricity generation and decolorization. After adding 800 mg/L sulfate, the active brilliant red X-3B (ABRX3) concentration in the effluent decreased from 208 to 67 mg/L and the maximum power density output increased by 20%. To quantify the reaction processes, a kinetics model based on a one-dimensional biofilm was developed. It showed that sulfur ions had a direct decolorization effect on ABRX3. The reaction of sulfide and ABRX3 at the anode was a first-order reaction. The decolorization and desulfurization mechanisms were validated by analyzing the microbial community at the anode. Sulfate-reducing bacteria (SRB) on the anode fermented the lactate to acetate. Then, electrogenic *Geobacter* used the acetate produced as a carbon source for electricity generation. The sulfide produced by SRB acted as additional fuel and a reductant and promoted the current generation and the reduction of azo bonds in the azo dye. Hence, the MFC showed potential for treating industrial textile wastewater.

*Keywords:* Azo dye wastewater; Microbial fuel cell; Model; Sulfate

### 1. Introduction

Textile wastewater contains high concentrations of bio-recalcitrant organics and toxic substances and is difficult to treat [1]. In the production of textiles, large amounts of sulfate and other inorganic salts are also added [2,3]. Sulfate in wastewater is reduced to sulfide by sulfate-reducing bacteria (SRB), which severely inhibits biodegradation in biological treatment devices [4,5]. In recent years, limits on sulfate concentrations have been proposed for the emission standards of China. Therefore, the simultaneous removal of sulfate and decolorization of textile wastewater should be emphasized.

A two-stage process is commonly adopted in commercial decolorization and desulfurization treatments. First, the sulfate is reduced to sulfide and blown off and then anaerobic decolorization treatment occurs in another reactor [6]. However, compared with traditional treatments, microbial fuel cells (MFCs) are better at degrading azo dyes via an extracellular electron transfer process [7]. Sun et al. [8] discovered that the decolorization of azo dye was increased to 95% compared with 80.1% with traditional anaerobic treatment. Microorganisms with extracellular electron transport capacity were enriched on the MFC anode. Compared with anaerobic treatment, anodes represent an extra electron acceptor and promote microbial metabolism [8]. Abundant outer membrane heme cytochromes, such as OmcC, OmcB, and MrtC, significantly promote the reduction of azo bonds

\*Corresponding author.

[9,10]. Recently, a combined MFC–photoelectrocatalytic cell system was established for the complete decolorization and degradation of azo dye [11,12]. Moreover, researchers also found that sulfate could be reduced to sulfite in MFCs and then oxidized into sulfur and deposited on the anode of the MFC [13]. Accordingly, we postulated that decolorization and sulfate removal could be achieved simultaneously at the MFC anode.

Although efforts have been made to improve the decolorization of dye in MFCs and sulfate conversion, little is known about the influence of sulfate conversion on decolorization and MFC current generation. As a strong reducing agent, sulfide can quickly break azo bonds. Yoo et al. [14] found that the sulfide produced from sulfate by *Desulfovibrio desulfuricans* rapidly decolorized the azo dyes C. I. Reactive Orange 96 and C. I. Reactive Red 120 under anaerobic conditions. Therefore, the conversion of sulfate could improve current generation and decolorization simultaneously in MFCs. Moreover, the synergistic metabolism of SRB and electroactive bacteria (EAB) found within MFCs should be elucidated to improve the treatment of textile wastewater. However, there is little information on the function and mechanism of sulfate in azo dye removal in MFCs.

This study used a two-chamber MFC for sulfate removal and the decolorization of active brilliant red X-3B (ABRX3). The relationship between sulfate conversion and decolorization is discussed. Microbial community analysis was used to clarify the mechanisms of simultaneous decolorization and desulfurization. In addition, a quantitative analysis of sulfate conversion and the promotion of dye decolorization were determined with a kinetic model.

## 2. Materials and methods

### 2.1. MFC fabrication and the inoculum

A two-chamber MFC made from Plexiglas was isolated using a cation-exchange membrane (Qianqiu Group, Zhejiang, China). The anode and cathode each had volumes of 70 mL. The anode was a graphite brush (Jinzhou Xinhaote, China) sealed with a rubber stopper. The cathode consisted of activated carbon (0.20–0.60 cm) and a stainless steel screen clamped in the middle of the activated carbon. The anode and cathode were connected by a copper wire. The MFC was inoculated with effluent from a constructed wetland MFC [11]. As the carbon source, 500 mg/L sodium acetate was added. The medium consisted of 0.3 g/L  $K_2HPO_4$ , 0.2 g/L  $KH_2PO_4$ , 1.0 g/L  $NH_4Cl$ , 0.1 g/L  $CaCl_2 \cdot 2H_2O$ , 0.1 g/L  $MgCl_2 \cdot 6H_2O$ , and 0.5 g/L  $FeSO_4 \cdot 7H_2O$ . One week later, the sludge from a secondary sedimentation tank, acclimated for 1 month to accumulate a sulfate-reducing consortium, was added to the MFC. The carbon source was changed from sodium acetate to sodium lactate.

### 2.2. Experiments

After a 1-month startup, batch experiments were conducted. The components of the artificial wastewater (anolyte) were as follows: 800 mg/L ABRX3, sodium lactate, 1183 mg/L  $Na_2SO_4$  (i.e., 800 mg/L  $SO_4$ ), 50 mmol/L phosphate buffer solution (PBS), 100 mg/L  $MgCl_2$ , 100 mg/L

$CaCl_2$ , and micronutrients [15]. The catholyte consisted of 50 mM PBS and was aerated throughout the experiment. Before the 36-h batch experiment, the anolyte was purged with nitrogen for 30 min. The test for sulfide oxidation in the MFC was conducted in an abiotic anode.

### 2.3. Analysis

The sulfate, lactate, and acetate concentrations in the samples were measured using ion chromatography (ICS-2100; Dionex, Bannockburn, IL, USA) after filtration (0.45  $\mu$ m). Each sample from the reactor was diluted 50-fold and then treated in an SPE tube (18 SPE tubes 3 mL; Supelco, USA). KOH gradient elution was used to separate anions in an IonPac AS19 guard column (4×50 mm) and an analytical column (4×250 mm). The methylene blue method was used to determine the sulfide concentration [16]. The ABRX3 decolorization efficiency was determined by measuring the absorbance at 540 nm (UV9100; Lab Tech, Beijing, China). The MFC current was recorded every 5 min with a data acquisition module (DAM-3210; Art Technology, China). Polarization curves were measured by regulating the external resistance from  $10^5$  to 5  $\Omega$ . Electrochemical impedance spectroscopy (EIS) of the MFC was performed at a frequency range from 100 kHz to 0.1 Hz. The EIS data were analyzed using ZSimpWin 3.10 software (EChem, USA) based on the equivalent electrical circuit [17]. The *t*-test was adopted according to previous work [18]. The microbial communities on the electrodes were determined using 16S rRNA high-throughput pyrosequencing [19].

### 2.4. Model development

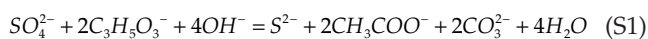
Starting with a previous one-dimensional biofilm model, we combined sulfate reduction and sulfide oxidation in the model. The model was developed based on four assumptions.

1. We ignored the anode microorganisms in the anolyte.
2. SRB metabolized the lactate.
3. EAB consumed the acetate at the MFC anode.
4. There was no concentration gradient in the main body of fluid.

#### 2.4.1. Reactions in the MFC anode

$S_i$  represented the concentration of component *i*.  $X_{SRB}$ ,  $X_{EAB}$  and  $X_{HO}$  were biomass corresponding to the sulfate, the lactate and the acetate transform process respectively. The units were in mg-N L<sup>-1</sup> for all nitrogenous species, mg-S L<sup>-1</sup> for all sulfur species, and mg-COD L<sup>-1</sup> for all organics.

Process 1: The Monod-type equation was used to describe the kinetics of the SRB metabolism. The SRB degraded lactate into acetate and yield biomass. The sulfate, as the electron acceptor, was reduced into the sulfide under anaerobic condition in the anode [Eq. (S1)]. Four kinetic expressions were described as follows:



$$\frac{dS_{SO_4^{2-}}}{dt} = \left( \frac{Y_{SRB} - 1}{1.875Y_{SRB}} \right) \frac{\mu_{SRB} S_{SO_4^{2-}}}{S_{SO_4^{2-}} + K_{SO_4^{2-}}^{SRB}} \frac{S_{C_3H_5O_3^-}}{S_{C_3H_5O_3^-} + K_{C_3H_5O_3^-}^{SRB}} X_{SRB} \quad (1)$$

$$\frac{dS_{S^{2-}}}{dt} = \frac{1 - Y_{SRB}}{Y_{SRB}} \frac{\mu_{SRB} S_{SO_4^{2-}}}{S_{SO_4^{2-}} + K_{SO_4^{2-}}^{SRB}} \frac{S_{C_3H_5O_3^-}}{S_{C_3H_5O_3^-} + K_{C_3H_5O_3^-}^{SRB}} X_{SRB} \quad (2)$$

$$\frac{dS_{C_3H_5O_3^-}}{dt} = -\frac{1}{Y_{SRB}} \frac{\mu_{SRB} S_{SO_4^{2-}}}{S_{SO_4^{2-}} + K_{SO_4^{2-}}^{SRB}} \frac{S_{C_3H_5O_3^-}}{S_{C_3H_5O_3^-} + K_{C_3H_5O_3^-}^{SRB}} X_{SRB} \quad (3)$$

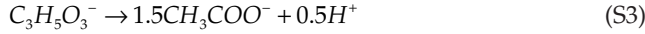
$$\frac{dS_{CH_3COO^-}}{dt} = \left( \frac{1 - Y_{SRB}}{1.5Y_{SRB}} \right) \frac{\mu_{SRB} S_{SO_4^{2-}}}{S_{SO_4^{2-}} + K_{SO_4^{2-}}^{SRB}} \frac{S_{C_3H_5O_3^-}}{S_{C_3H_5O_3^-} + K_{C_3H_5O_3^-}^{SRB}} X_{SRB} \quad (4)$$

Process 2: EABs degraded the acetate [Eq. (S2)]. The kinetic expression was stated as follows:



$$\frac{dS_{CH_3COO^-}}{dt} = -\frac{\mu_{EAB}}{Y_{EAB}} \frac{S_{CH_3COO^-}}{S_{CH_3COO^-} + K_{CH_3COO^-}^{EAB}} X_{EAB} \quad (5)$$

Process 3: Facultative bacteria competed lactate with SRB [Eq. (S3)]. The kinetic expression for this process was as follows:



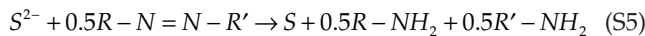
$$\frac{dS_{CH_3COO^-}}{dt} = -\frac{\mu_{FB}}{Y_{FB}} \frac{S_{C_3H_5O_3^-}}{S_{C_3H_5O_3^-} + K_{C_3H_5O_3^-}^{HO}} X_{FB} \quad (6)$$

Process 4: The anode of MFC oxidized  $S^{2-}$  (Eq. (S4)).



$$\frac{dS^{2-}}{dt} = -K_{electrode} \times S^{2-} \quad (7)$$

Process 5: Azo dye was reduced by  $S^{2-}$  (Eq. (S5)).



$$\frac{dS^{2-}}{dt} = -K_{S^{2-}} \times S^{2-} \quad (8)$$

Process 6: Azo dye anaerobic biological decolorization in MFC

Bio-recalcitrant organics degradation is achieved by enzyme excreted by organism and the bioelectrochemical reaction. It is difficult to describe the process by a Monod-type equation. According to the profile of ABRX3 concentration during the degradation, The first-order kinetic equation was chosen to describe the decolorization in MFC anode.

$$\frac{dS^{2-}}{dt} = -K_{microorganism} \times S^{2-} \quad (9)$$

#### 2.4.2. Kinetic parameters of mathematical model

Under anaerobic conditions, SRB use volatile organic acids as electron donors to reduce sulfate. SRB with the ability to oxidize lactate rather than acetate predominate when sufficient lactate is supplied as the carbon source [24]. In addition, the specific growth rate of SRB oxidizing lactate is faster than that of SRB oxidizing acetate. In this study, lactate was provided at high concentrations and rapid desulfurization was observed. The process of sulfate reduction is described in Eq. (S1); possible acetate oxidation by SRB was ignored. Most of the EAB, such as *Geobacter metallireducens* and *Geobacter sulfurreducens*, could metabolize only acetate and not lactate or other complex organic compounds [25]. *Geobacter* was the dominant species in the inoculation, as we confirmed previously [26]. Therefore, to simplify Process 2, the consumption of lactate by EAB was ignored, and we considered only the consumption of acetate by bacteria. Nevertheless, the extracellular electron transfer ability of some SRB was ruled out because the sulfate concentration remained static after running out of lactate (as shown in Fig. 3).

The model parameters regarding EAB (Eqs. (S2), (5)) were obtained from Moosa et al. and Xu et al. [20,27]. The parameters for sulfide oxidation at the anode and consumption by azo dye were acquired by fitting the data with a first-order kinetic equation. The model parameters for sulfate reduction (Eqs. (S1), (1)–(4)) were estimated.

### 3. Results and discussion

#### 3.1. Model fitting

Fig. 1A shows the current output by the MFC that consumed sulfide as the only electron donor. As soon as the circuit was closed, the current immediately increased to 0.35 and 0.58 mA at 1000 and 500  $\Omega$ , respectively. Over the first 3 h, the current increased slightly to 0.48 and 0.67 mA, respectively, and then decreased gradually to 0.28 and 0.33 mA after 24 h. Compared with 1000  $\Omega$ , the 500  $\Omega$  resistor increased the total current output. Fig. 1B shows the sulfide removal in the MFC. First-order kinetics described the sulfide removal. The kinetic constants for sulfide removal at 1000 and 500  $\Omega$  were 0.049  $h^{-1}$  ( $R^2 = 0.992$ ) and 0.060  $h^{-1}$  ( $R^2 = 0.997$ ), respectively, which corresponded to the current output in Fig. 1A.

Dutta et al. [28] developed a similar reactor and found that, compared with 50  $\Omega$ , the current at 10  $\Omega$  improved 4-fold. When the external resistance was decreased, the current approached the limit of the anode. Essentially, the current reflected the sulfide oxidation reaction rate at the anode, with a higher current corresponding to a higher sulfide removal rate. The anodic microbial film does not appear to retard the oxidation of sulfur ions at the anode [13]. Therefore, the kinetic constants of sulfide removal determined here can be used when the biofilm is attached to the surface of the anode. Oxidation from sulfide to other high-valence states in this MFC was ignored because of the extremely low concentration of oxygen as the electron acceptor at the anaerobic anode [29,30]. In general, the first-order kinetic constant of sulfide oxidation represented the reaction at the anode.

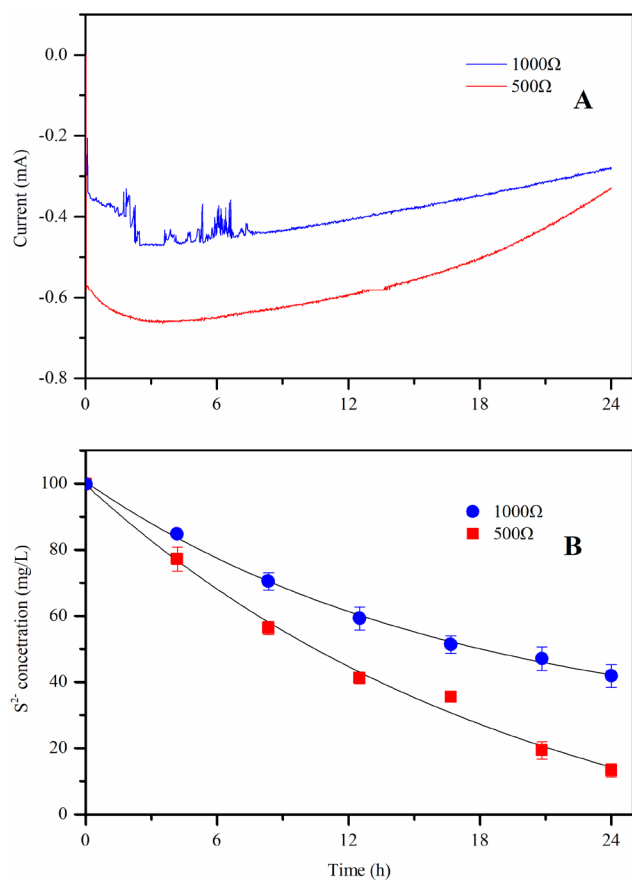


Fig. 1. Sulfide reduction at the electrode. (A) Time–current curves of the MFC with sulfide as the only electron donor. (B) The evolution of sulfide oxidation at 500 and 1000  $\Omega$  during a batch period.

As shown in Fig. 2A, the Absorption of ABRX3 with different ratios of added sulfide decreased gradually. When the ratio was 4.2:1, there was little attenuation of the ABS. As sulfide reduced ABRX3, we chose a mass ratio of 4.2:1. Fig. 2B describes the decolorization of ABRX3 in the MFC. After 36 h, the ABRX3 concentration decreased from 800 to ~230 mg/L at resistances of both 500 and 1000  $\Omega$ , with no significant difference between the two tested resistances ( $P > 0.05$ ,  $t$ -test). Therefore, the same first-order kinetic constant ( $0.041 \text{ h}^{-1}$ ,  $R^2 = 0.9837$ ) was fitted in this study.

The rapid chemical decolorization of azo dye with sulfide has been reported in an anaerobic reactor [14,31]. It has been proven that sulfide had no influence on electricity production, even at a concentration of ~200 mg/L [13]. The maximum theoretical sulfide concentration in this experiment was ~200 mg/L. Therefore, the toxic effects on microorganism metabolism and decolorization at the anode were ignored. Although no sulfate was added at the anode in this test, this kinetic constant was still used when sulfate was added.

A previous study concluded that low resistance favored the removal of ABRX3. However, the difference in removal efficiency was minimal, as shown in Fig. 2B. The mechanism for accelerating decolorization in the MFC was as follows: the graphite brush functioned as an electron acceptor

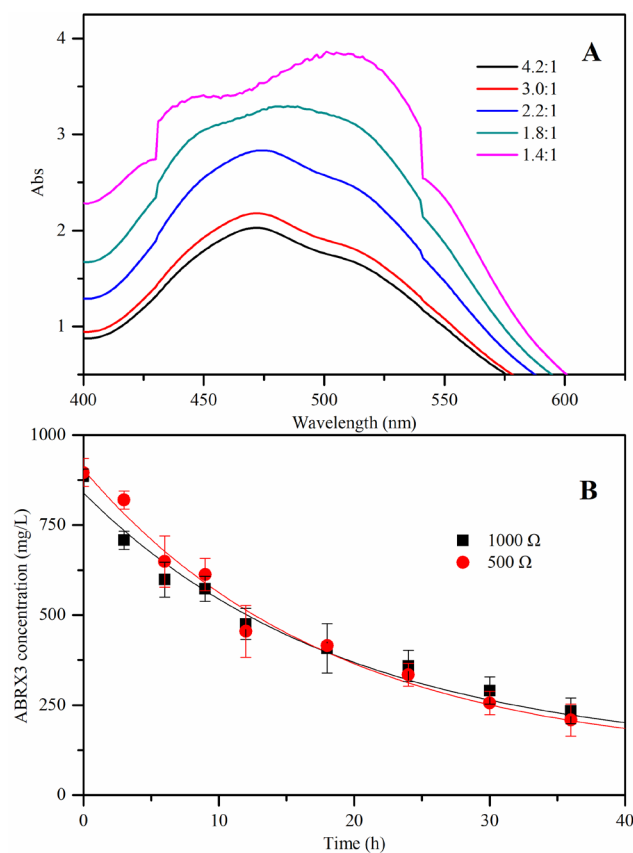


Fig. 2. Efficiency of decolorization by sulfide and the MFC without added sulfate. (A) Ultraviolet–visible absorbance for different ratios of sulfide to ABRX3. (B) ABRX3 decolorization in the MFC without sulfate addition over 36 h.

and was sufficient for microorganism metabolism, facilitating the generation of electrons and reduction of the azo dye [8,32]. In our experiment, the high lactate concentration provided sufficient electron donors for breaking the azo bonds. Therefore, no acceleration at the anode was evident.

Based on the equations in Processes 1–4, the experimental data and fitting results are depicted in Fig. 3A. During the first 9 h, lactate was consumed and transformed into acetate, which corresponded to the drop in the sulfate concentration. Then, the acetate concentration slowly decreased to ~600 mg/L, while the sulfate concentration was maintained at ~170 mg/L. The coulombic efficiency was 8.78%. The current came from both the sulfide oxidation and the *Geobacter* extracellular electron transfer. It may not accurate to certified the contribution of the sulfide oxidation and the *Geobacter* to the current generation and the electron donor.

Based on the experimental results when using 2500 mg/L lactate (Fig. 3A), the SRB biomass density ( $\rho_{SRB}$ ), SRB initial volume fraction ( $R_{SRB}$ ), and yield coefficient ( $Y_{SRB}$ ) were estimated to fit Eq. (S1), and the initial EAB volume fraction ( $R_{EAB}$ ) and initial FB volume fraction ( $R_{FB}$ ) were estimated based on the sensitivity ranking of parameters in the supporting information. Table 1 lists the revised values of the kinetic and stoichiometric parameters used in our model.

Given the rapid sulfate removal rate, a 58% initial volume fraction of SRB was obtained by parameter estimation.

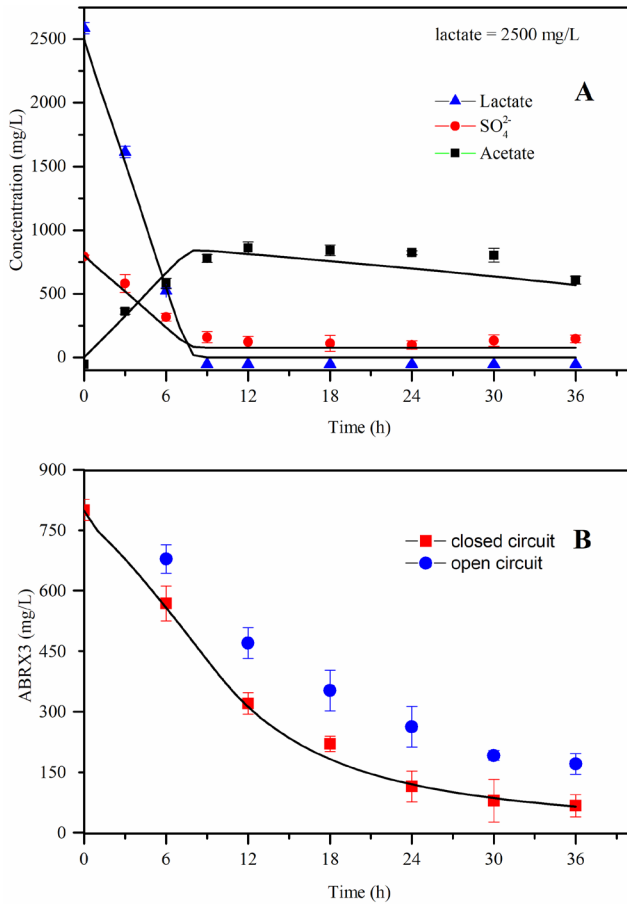


Fig. 3. Model fitting of the results of the sulfate reduction, sulfide oxidation, acetate oxidation, and ABRX3 decolorization equations to the experimental data at lactate = 2500 mg/L. The solid line represents the simulated result and the points the experimental data.

According to a previous study [20], *Desulfobulbus*, a typical incomplete-oxidation SRB, accounted for 24% of the relative abundance when oxygen was fed into the reactor. The lack of oxygen may have resulted in the high initial volume fraction.

Fig. 3B plots the decolorization of ABRX3. The ABRX3 concentration decreased from 800 to 66.7 mg/L. As incomplete oxidizers, the SRB in the MFC anode degraded the lactate into acetate and reduced the sulfate into sulfide. In previous work, this conversion process usually continued for 1–5 d [33]. The rapid rate of sulfate reduction in our work was attributed to the huge area of the graphite brush compared with carbon felt. The significant improvement of 133 mg/L ABRX3 decolorization was attributed to the reduction by the sulfide from the sulfate reduction.

3.2. Sensitivity analysis of the parameters

Fig. 4 shows the sensitivities of the model parameters for lactate consumption. As shown in Fig. 4A, the rate of lactate consumption decreased as the  $\rho_{SRB}$  value increased. Figs. 4B and C show the respective effects of  $Y_{SRB}$  and  $R_{SRB}$

Table 1 Kinetic and stoichiometric parameters of anode reaction

Parameter	Definition	Value	References
$\mu_{SRB}$	Maximum specific growth rate of SRB, h <sup>-1</sup>	0.061	[19]
$K_{SO_4 SRB}$	Sulfate affinity constant for SRB, mg S L <sup>-1</sup>	3.85	Measured
$K_{lactate SRB}$	Lactate affinity constant for SRB, mg COD L <sup>-1</sup>	18.5	[19]
$\mu_{EAB}$	Maximum specific growth rate of EAB, h <sup>-1</sup>	0.02	Assumed
$K_{acetate EAB}$	Sulfate affinity constant for EAB, mg COD L <sup>-1</sup>	150	[20]
$\mu_{FB}$	Maximum specific growth rate of FB, h <sup>-1</sup>	0.18	[19]
$K_{lactate FB}$	Lactate affinity constant for SRB, mg COD L <sup>-1</sup>	20	[19]
$K_{micro}$	First-order kinetic of microorganism decolorization, h <sup>-1</sup>	0.035	Measured
$K_s$	First-order kinetic for sulfide oxidation by azo dye, h <sup>-1</sup>	0.047	Measured
$K_{electrode}$	First-order kinetic for sulfide oxidation by the electrode, h <sup>-1</sup>	0.065	Measured
$b_{SRB}$	Endogenous decay rate of SRB, h <sup>-1</sup>	0.035	[19]
$b_{EAB}$	Endogenous decay rate of EAB, h <sup>-1</sup>	0.00083	[21]
$b_{FB}$	Endogenous decay rate of FB, h <sup>-1</sup>	0.0258	[19]
$Y_{SRB}$	Yield coefficient for SRB, g VSS g <sup>-1</sup> COD	0.458	Measured
$Y_{EAB}$	Yield coefficient for EAB, g VSS g <sup>-1</sup> COD	0.212	[22]
$Y_{FB}$	Yield coefficient for FB, g VSS g <sup>-1</sup> COD	0.67	[19]
$\rho_{SRB}$	The SRB biomass density in biofilm, mg/L	86912	Measured
$R_{SRB}$	The SRB volume fraction in biofilm	58%	Measured
$P_{EAB}$	The EAB biomass density in biofilm, mg/L	64200	Assumed
$R_{EAB}$	The EAB volume fraction in biofilm	3%	Measured
$P_{FB}$	The FB biomass density in biofilm, mg/L	64200	Assumed
$R_{FB}$	The FB volume fraction in biofilm	4.6%	Measured
$A$	The area of biofilm, m <sup>2</sup>	0.104	Measured
$V$	The volume of anode chamber, cm <sup>3</sup>	70	Measured

on the configuration file. The rate of lactate consumption increased with  $Y_{SRB}$ . At high values of  $R_{SRB}$  and  $\rho_{SRB}$ , the effect on the lactate consumption rate was minimal. Conversely, when  $R_{SRB}$  and  $\rho_{SRB}$  decreased, the lactate consumption rate changed significantly.

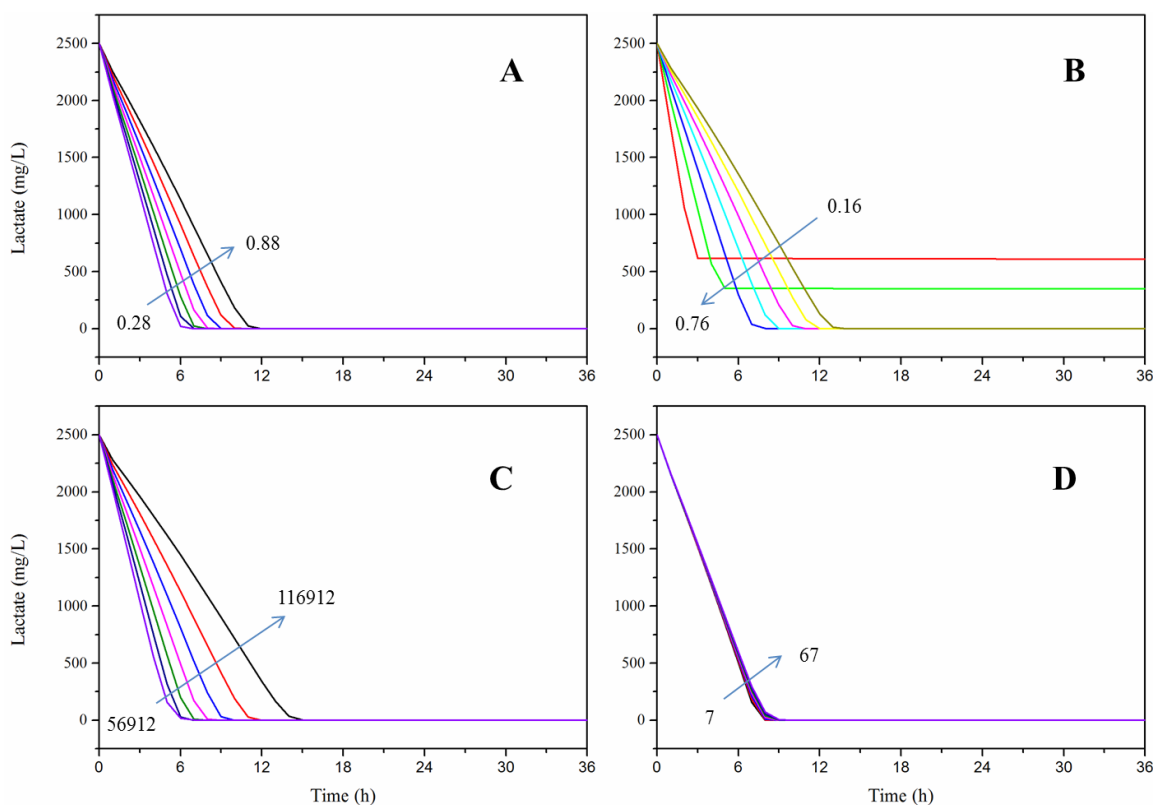


Fig. 4. Sensitivity of the parameters for lactate consumption: (a)  $\rho_{SRB'}$  (b)  $Y_{SRB'}$  (c)  $R_{SRB'}$  and (d)  $K_{lactate}$ .

$Y_{SRB}$  represents the electron distribution of cell metabolism [34]. A high  $Y_{SRB}$  resulted in a lower lactate consumption rate. However, a low  $Y_{SRB}$  could not satisfy the balance between synthesis and decomposition, leading to the death of the SRB (Fig. 4B). In this study, the density and initial ratio of the SRB biofilm could be fitted by the data because of the high sensitivity. The significant deviation of a profiles implied high sensitivity of  $R_{SRB}$  and  $\rho_{SRB'}$  which could be determined by the parameter estimation according to the supporting information. Compared with the other parameters,  $K_{lactate}$  had less effect on the lactate consumption (Fig. 4D).

### 3.3. Pollutant removal performance and power generation

Fig. 5A shows the decolorization efficiency under different lactate concentrations. Of the three lactate concentrations, the best decolorization occurred at 2000 mg/L. An 80 mg/L decrease at 36 h was observed, which was attributed to sulfate reduction. By oxidizing lactate to acetate, the SRB utilized sufficient electrons to produce sulfide. Therefore, better decolorization efficiency was acquired because there was sufficient sulfide corresponding to the higher lactate concentration.

Figs. 5B–D show the evolution of sulfate, lactate, and acetate in the MFC. After the rapid exhaustion of lactate, acetate accumulated. Then, the acetate concentration decreased. As the lactate concentration decreased, more sulfate was maintained in the MFC. A lactate dosage of 2000 mg/L resulted in 250 mg/L sulfate after 36 h, whereas

the acetate concentration decreased to 363 mg/L. The respective sulfate and acetate concentrations were 431 and 213 mg/L with an initial concentration of 1500 mg/L lactate, and 500 and 117 mg/L with 1000 mg/L lactate. The high concentrations of electron donors provided sufficient electrons for the reduction of sulfate. As shown in Fig. 4, the final concentration of sulfate decreased, while the lactate concentration increased. After the depletion of lactate, the sulfate concentration remained constant, which indicated that the SRB oxidizing lactate to acetate predominated in the MFC. Therefore, the simplification of sulfate reduction in the model in this study was suitable. The capacity of the model to describe the sulfate transformation and decolorization kinetics in our MFC with the estimated-revised parameters confirmed the validity of the model (Fig. 5).

Fig. 6 shows the power output characteristics. The maximum power density decreased by 20% without added sulfate. The power output of the MFC in this experiment was related not only to the EAB but also to the sulfate. The sulfide was oxidized at the anode and released electrons, increasing the current output. A difference was observed in the Nyquist plot, as shown in Fig. 6B. By fitting data with an equivalent circuit R(CR)(QR), resistances were acquired. The ohmic, cathode, and anode resistances were 115.4, 28.2, and 164.9  $\Omega$ , respectively. After adding sulfate, the resistances changed to 90, 29.4, and 136.2  $\Omega$ , respectively. The decrease in ohmic resistance may have resulted from the increased conductivity caused by the addition of 800 mg/L sulfate. Nevertheless, the resistance of the

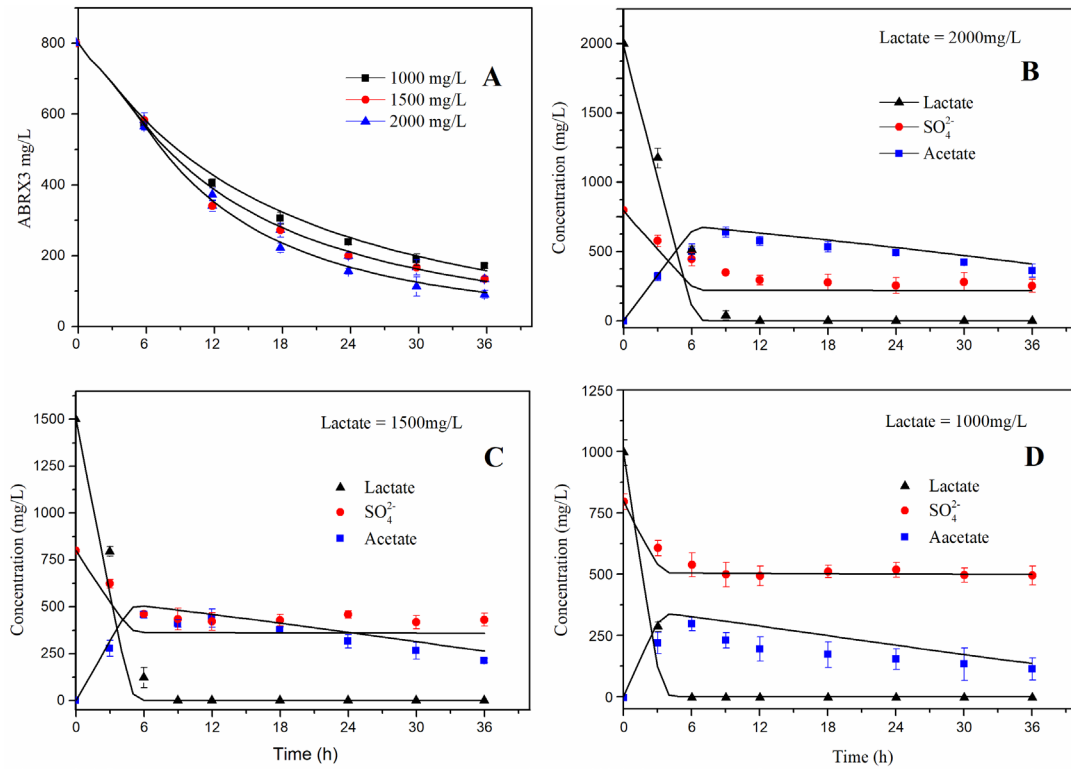


Fig. 5. Model fitting results for the ABRX3 decolorization, lactate oxidation, sulfate reduction, and acetate production equations to the experimental data at different initial lactate concentrations. The solid lines are the model-fitting curves. Figs. 5 B–D correspond to initial lactate concentrations of 2000, 1500, and 1000 mg/L, respectively.

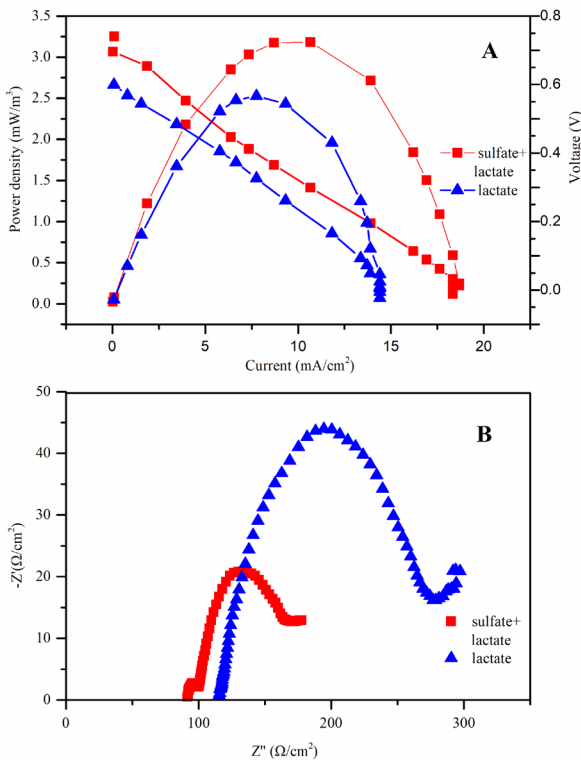


Fig. 6. Power output characteristics under different resistors. (A) Polarization curve of the MFC. (B) Nyquist plot of the MFC.

anode also decreased. Therefore, by reducing the anode and ohmic resistances, the power output was increased by adding sulfate.

### 3.4. Mechanisms of decolorization and desulfurization at the MFC anode

The microbial community was analyzed to validate the reactions proposed in the kinetic model and to elucidate the mechanism of the simultaneous decolorization and desulfurization in this study. Eight bacterial genera with relative abundances >1% were discovered in the anode (Fig. 7A). Three SRB predominated: *Desulfovibrio* (7.51%), *Macellibacteroides* (11.0%), and *Veillonella* (32.7%). *Desulfovibrio* is commonly found in aquatic environments with high levels of organics and sulfate, and is regarded as the main SRB [35]. *Macellibacteroides* separated from an upflow anaerobic filter treating abattoir wastewater was also proved to reduce sulfate [36]. *Veillonella* has also been shown to reduce sulfate [37]. Note that all three genera of bacteria showed incomplete fermentation capacity, and used lactate as a carbon source rather than acetate. In addition, *Geobacter* (5.11%), a typical anaerobic species with the strongest current generation capacity, was observed in the anode. *Geobacter* is reported to use only acetate as carbon source [38]. Therefore, in this study, SRB initially fermented lactate to produce acetate, and the SRB reduced sulfate, as an electron acceptor, into sulfide. Then, the acetate was used as a carbon source to generate electricity. The current came from both

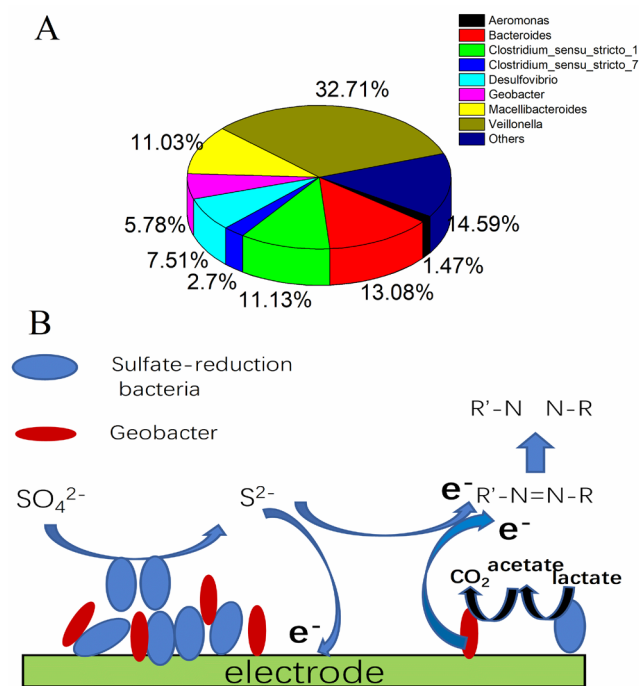


Fig. 7. Mechanisms of decolorization and desulfurization at the anode. (A) Taxonomy of the microbial community classified at the genus level. (B) Schematic diagram of the reactions at the bioanode.

sulfide oxidation and *Geobacter* extracellular electron transfer. The total relative abundance of SRB was 51.5%, while that of electrogenic bacteria was 5.7%, which were near the parameters proposed for our kinetic model. Therefore, the kinetic model and mechanism of the reactions proposed were accurate and can guide the treatment of textile wastewater in MFCs.

#### 4. Conclusion

Simultaneous ABRX3 decolorization and sulfur removal were achieved in one MFC for the first time. The influence of different concentrations of sulfate on MFC power generation and decolorization was assessed by establishing a mathematical model to describe the kinetic processes. The rapid reduction of sulfate to sulfide led to a 15% increase in the MFC power density and the decolorization rate increased from 74% to 91%. Therefore, the MFC described here has the potential for decolorizing azo dyes and removing sulfate in textile wastewater simultaneously.

#### Acknowledgments

This work was supported by the Provincial Natural Science Foundation of Jiangsu, China [BK20171351], the National Natural Science Foundation of China [21277024], the Fundamental Research Funds for the Central Universities [2242016K41042], the Scientific Research Foundation of Graduate School of Southeast University and the JSPS KAKENHI [Grant Numbers JP16H02747] for financial support.

#### References

- [1] M. Bayramoglu, M. Kobya, O.T. Can, M. Sozbir, Operating cost analysis of electrocoagulation of textile dye wastewater, *Separ. Purif. Technol.*, 37 (2004) 117–125.
- [2] P.C. Vandevivere, R. Bianchi, W. Verstraete, Treatment and reuse of wastewater from the textile wet-processing industry: review of emerging technologies, *Cheminform.*, 29 (1998).
- [3] B. Manu, S. Chaudhari, Anaerobic decolorisation of simulated textile wastewater containing azo dyes, *Bioresour. Technol.*, 82 (2002) 225–231.
- [4] D.M. McCartney, J.A. Oleszkiewicz, Sulfide inhibition of anaerobic degradation of lactate and acetate, *Water Res.*, 25 (1991) 203–209.
- [5] Y. Gao, Anaerobic digestion of high strength wastewaters containing high levels of sulphate: University of Newcastle upon Tyne; 1989.
- [6] C.H. Wei, W.X. Wang, Z.Y. Deng, C.F. Wu, Characteristics of high-sulfate wastewater treatment by two-phase anaerobic digestion process with Jet-loop anaerobic fluidized bed, *J. Environ. Sci.*, 19 (2007) 264–270.
- [7] H. Rismaniyazdi, A.D. Christy, S.M. Carver, Z.T. Yu, B.A. Dehority, O.H. Tuovinen, A. Pandey, D.J. Lee, B.E. Logan, Effect of external resistance on bacterial diversity and metabolism in cellulose-fed microbial fuel cells, *Bioresour. Technol.*, 102 (2011) 278–283.
- [8] J. Sun, Z. Bi, B. Hou, Y.Q. Cao, Y.Y. Hu, Further treatment of decolorization liquid of azo dye coupled with increased power production using microbial fuel cell equipped with an aerobic biocathode, *Water Res.*, 45 (2011) 283–291.
- [9] Y.-N. Liu, F. Zhang, J. Li, D.-B. Li, D.-F. Liu, W.-W. Li, H.-Q. Yu, Exclusive extracellular bioreduction of methyl orange by azo reductase-free *Geobacter* sulfur reducers, *Environ. Sci. Technol.*, 51 (2017) 8616–8623.
- [10] P.-J. Cai, X. Xiao, Y.-R. He, W.-W. Li, J. Chu, C. Wu, M.-X. He, Z. Zhang, G.-P. Sheng, M.H.-W. Lam, Anaerobic biodecolorization mechanism of methyl orange by *Shewanella oneidensis* MR-1, *Appl. Microbiol. Biotechnol.*, 93 (2012) 1769–1776.
- [11] X. Long, Q. Pan, C. Wang, W. Hui, L. Hua, X. Li, Microbial fuel cell-photoelectrocatalytic cell combined system for the removal of azo dye wastewater, *Bioresour. Technol.*, 244 (2017) 182–191.
- [12] X. Long, H. Wang, C. Wang, X. Cao, X. Li, Enhancement of azo dye degradation and power generation in a photoelectrocatalytic microbial fuel cell by simple cathodic reduction on titanium nanotube arrays electrode, *Journal of Power Sources*, 415 (2019) 145–153.
- [13] D.-J. Lee, C.-Y. Lee, J.-S. Chang, Q. Liao, A. Su, Treatment of sulfate/sulfide-containing wastewaters using a microbial fuel cell: single and two-anode systems, *Int. J. Green Energy*, 12 (2014) 998–1004.
- [14] E.S. Yoo, J. Libra, U. Wiesmann, Reduction of azo dyes by *Desulfovibrio desulfuricans*, *Water Sci. Technol.*, 41 (2000) 15.
- [15] Y. Li, A. Lu, H. Ding, X. Wang, C. Wang, C. Zeng, Y. Yan, Microbial fuel cells using natural pyrrhotite as the cathodic heterogeneous Fenton catalyst towards the degradation of biorefractory organics in landfill leachate, *Electrochem. Commun.*, 12 (2010) 944–947.
- [16] X. Xu, C. Chen, A. Wang, W. Guo, X. Zhou, D.J. Lee, N. Ren, J.S. Chang, Simultaneous removal of sulfide, nitrate and acetate under denitrifying sulfide removal condition: modeling and experimental validation, *J. Hazard. Mater.*, 264 (2014) 16–24.
- [17] Y. Du, Y. Qu, X. Zhou, Y. Feng, Electricity generation by biocathode coupled photoelectrochemical cells, *RSC Adv.*, 5 (2015) 25325–25328.
- [18] W. Haynes, Student's t-Test. *Encyclopedia of Systems Biology*: Springer; 2013, p. 2023–2025.
- [19] X. Ying, D. Shen, M. Wang, H. Feng, Y. Gu, W. Chen, Titanium dioxide thin film-modified stainless steel mesh for enhanced current-generation in microbial fuel cells, *Chem. Eng. J.*, 333 (2018) 260–267.

- [20] X.J. Xu, C. Chen, A.J. Wang, B.J. Ni, W.Q. Guo, Y. Yuan, C. Huang, X. Zhou, D.H. Wu, D.J. Lee, N.Q. Ren, Mathematical modeling of simultaneous carbon-nitrogen-sulfur removal from industrial wastewater, *J. Hazard. Mater.*, 321 (2017) 371–381.
- [21] S. Ou, H. Kashima, D.S. Aaron, J.M. Regan, M.M. Mench, Full cell simulation and the evaluation of the buffer system on air-cathode microbial fuel cell, *J. Power Sources*, 347 (2017) 159–169.
- [22] Z.Z. Ismail, A.A. Habeeb, Experimental and modeling study of simultaneous power generation and pharmaceutical wastewater treatment in microbial fuel cell based on mobilized biofilm bearers, *Renew. Energy*, 101 (2017) 1256–1265.
- [23] M. Esfandyari, M.A. Fanaei, R. Gheshlaghi, M.A. Mahdavi, Mathematical modeling of two-chamber batch microbial fuel cell with pure culture of *Shewanella*, *Chem. Eng. Res. Design*, 117 (2017) 34–42.
- [24] O.J. Hao, J.M. Chen, L. Huang, R.L. Buglass, Sulfate-reducing bacteria, *Handbook of Water & Wastewater Microbiol.*, 26 (2003) 459–469.
- [25] C. Ma, S. Zhou, L. Zhuang, C. Wu, Electron transfer mechanism of extracellular respiration: A review, *Acta Ecologica Sinica*, 31 (2011) 2008–2018.
- [26] T. Li, Z. Fang, R. Yu, X. Cao, H. Song, X. Li, The performance of the microbial fuel cell-coupled constructed wetland system and the influence of the anode bacterial community, *Environ. Technol.*, 37 (2016) 1683–1692.
- [27] S. Moosa, M. Nemati, S.T.L. Harrison, A kinetic study on anaerobic reduction of sulphate, Part I: Effect of sulphate concentration, *Chem. Eng. Sci.*, 57 (2002) 2773–2780.
- [28] P.K. Dutta, K. Rabaey, Z. Yuan, J. Keller, Spontaneous electrochemical removal of aqueous sulfide, *Water Res.*, 42 (2008) 4965–4975.
- [29] F. Zhao, N. Rahunen, J.R. Varcoe, A.J. Roberts, C. Avignone-Rossa, A.E. Thumser, R.C. Slade, Factors affecting the performance of microbial fuel cells for sulfur pollutants removal, *Biosens. Bioelectron.*, 24 (2009) 1931–1936.
- [30] X. Xu, C. Chen, D.J. Lee, A. Wang, W. Guo, X. Zhou, H. Guo, Y. Yuan, N. Ren, J.S. Chang, Sulfate-reduction, sulfide-oxidation and elemental sulfur bioreduction process: modeling and experimental validation, *Bioresour. Technol.*, 147 (2013) 202–211.
- [31] E.S. Yoo, J. Libra, L. Adrian, Mechanism of decolorization of azo dyes in anaerobic mixed culture, *J. Environ. Eng.*, 127 (2001) 844–849.
- [32] J.M. Morris, S. Jin, B. Crimi, A. Pruden, Microbial fuel cell in enhancing anaerobic biodegradation of diesel, *Chem. Eng. J.*, 146 (2009) 161–167.
- [33] D.J. Lee, X. Liu, H.L. Weng, Sulfate and organic carbon removal by microbial fuel cell with sulfate-reducing bacteria and sulfide-oxidising bacteria anodic biofilm, *Bioresour. Technol.*, 156 (2014) 14–19.
- [34] B.J. Ni, F. Fang, W.M. Xie, M. Sun, G.P. Sheng, W.H. Li, H.Q. Yu, Characterization of extracellular polymeric substances produced by mixed microorganisms in activated sludge with gel-permeating chromatography, excitation–emission matrix fluorescence spectroscopy measurement and kinetic modeling, *Water Res.*, 43 (2009) 1350–1358.
- [35] J. Odom, H. Peck Jr, Hydrogen cycling as a general mechanism for energy coupling in the sulfate-reducing bacteria, *Desulfovibrio* sp, *FEMS Microbiol. Lett.*, 12 (1981) 47–50.
- [36] L. Jabari, H. Gannoun, J.-L. Cayol, A. Hedi, M. Sakamoto, E. Falsen, M. Ohkuma, M. Hamdi, G. Fauque, B. Ollivier, *Macellibacteroides fermentans* gen. nov., sp. nov., a member of the family Porphyromonadaceae isolated from an upflow anaerobic filter treating abattoir wastewaters, *Int. J. Syst. Evol. Microbiol.*, 62 (2012) 2522–2527.
- [37] H.J. Laanbroek, H.J. Geerligs, A.A. Peijnenburg, J. Siesling, Competition for L-lactate between *Desulfovibrio*, *Veillonella*, and *Acetobacterium* species isolated from anaerobic intertidal sediments, *Microb. Ecol.*, 9 (1983) 341–354.
- [38] H. Yi, K.P. Nevin, B.-C. Kim, A.E. Franks, A. Klimes, L.M. Tender, D.R. Lovley, Selection of a variant of *Geobacter sulfurreducens* with enhanced capacity for current production in microbial fuel cells, *Biosens. Bioelectron.*, 24 (2009) 3498–3503.